

# Charged Gravastars in Rastall-Rainbow Gravity

Ujjal Debnath\*

Department of Mathematics,  
Indian Institute of Engineering Science and Technology,  
Shibpur, Howrah-711 103, India.

In this work, we have considered the spherically symmetric stellar system in the contexts of Rastall-Rainbow gravity theory in presence of isotropic fluid source with electro-magnetic field. The Einstein-Maxwell's field equations have been written in the framework of Rastall-Rainbow gravity. Next we have discussed the geometry of charged gravastar model. The gravastar consists of three regions: interior region, thin shell region and exterior region. In the interior region, the gravastar follows the equation of state (EoS)  $p = -\rho$  and we have found the solutions of all physical quantities like energy density, pressure, electric field, charge density, gravitational mass and metric coefficients. In the exterior region, we have obtained the exterior Riessner-Nordstrom solution for vacuum model ( $p = \rho = 0$ ). Since in the shell region, the fluid source follows the EoS  $p = \rho$  (ultra-stiff fluid) and the thickness of the shell of the gravastar is infinitesimal, so by the approximation  $h (\equiv A^{-1}) \ll 1$ , we have found the analytical solutions within the thin shell. The physical quantities like the proper length of the thin shell, entropy and energy content inside the thin shell of the charged gravastar have been computed and we have shown that they are directly proportional to the proper thickness of the shell ( $\epsilon$ ) due to the approximation ( $\epsilon \ll 1$ ). The physical parameters significantly depend on the Rastall parameter and Rainbow function. Next we have studied the matching between the surfaces of interior and exterior regions of the charged gravastar and using the matching conditions, the surface energy density and the surface pressure have been obtained. Also the equation of state parameter on the surface, mass of the thin shell, mass of the gravastar have been obtained. Finally, we have explored the stable regions of the charged gravastar in Rastall-Rainbow gravity.

## I. INTRODUCTION

A *gravastar* is astronomically hypothetical condensed object which is a gravitationally dark cold vacuum compact star or gravitational vacuum condensate star. Mazur and Mottola [1, 2] have established the gravastar solution in the concept of Bose-Einstein condensation to gravitational systems. The gravastar is singularity free object which is spherically symmetric as well as super compact. It has also the property that it has no event horizon. So the gravastar is a substitute of black hole i.e., the existence of compact stars minus event horizons. The gravastar consists of three regions: (i) *Interior region* ( $0 \leq r < r_1$ ), (ii) *Shell region* ( $r_1 < r < r_2$ ) and (iii) *Exterior region* ( $r_2 < r$ ), where  $r_1$  and  $r_2$  are inner and outer radii ( $r_1 < r_2$ ). In the interior region, the isotropic pressure produces a force of repulsion over the intermediate thin shell. So the equation of state (EOS) of the fluid satisfies  $p = -\rho$  which describes the de-Sitter spacetime. The intermediate thin shell region consists of ultra-stiff perfect fluid satisfies the EoS  $p = \rho$ . The exterior region consists of vacuum with EOS  $p = \rho = 0$  which is described by the Schwarzschild solution. Visser [3] developed the mathematical model of the gravastar and described the stability of gravastar by taking some realistic values of EoS parameter.

DeBenedictis et al [4] have found the gravastar solutions by taking continuous pressures and the equation of state. The anisotropic pressure for the structure of gravastar has

been considered by Cattoen et al [5]. Bilic et al [6] have found the gravastar solution in presence of Born-infeld phantom model. Carter [7] studied the stability of the gravastar. The Gravastar solutions in the framework of conformal motion have been investigated by some authors [8–10]. Gravastar model in higher dimensional spacetime has been discussed in refs [9, 11–13]. Several authors [14–20] have discussed the stable nature of gravastars. Charged gravastar models with its physical features have been analyzed in the works [8, 9, 12, 21–28]. Ray et al [29] have described the charged strange quark star model in the framework of electromagnetic mass with conformal killing vector.

In the framework of modified gravity theory, lot of works on compact star, neutron star, strange star and gravastar have been found in the literature. Boehmer et al [30] have examined the existence of relativistic stars in  $f(T)$  modified gravity. The structure of neutron stars in modified  $f(T)$  gravity has been studied by Deliduman et al [31]. In refs [32, 33], the authors have studied the anisotropic strange stars in  $f(T)$  gravity model. The structures of relativistic stars in  $f(T)$  gravity and its Tolman-Oppenheimer-Volkoff (TOV) equations have been computed in [34]. In  $f(T)$  gravity model, the compact star models have been studied in [35] and the neutron star models have been discussed in [36]. Using the Krori and Barua (KB) metric [37], the anisotropic compact star models in GR,  $f(R)$ ,  $f(G)$  and  $f(T)$  theories have been studied in refs [38–41]. The gravastar solution in  $f(R, T)$  gravity model has been studied in [42, 43]. Also the Gravastar solution in  $f(G, T)$  gravity model has been found in [44].

---

\*ujjaldebnath@gmail.com

Rastall gravity theory is proposed by Rastall [45], which is one of the alternative of modified gravity theory by modification the Einstein's general relativity. Neutron Stars in Rastall Gravity have been obtained by Oliveira et al [46]. A model of quintessence compact stars in the Rastall's theory of gravity has been obtained by Abhas et al [47]. Isotropic compact star model in Rastall theory admitting conformal motion has also been obtained in [48]. Anisotropic compact star model in the Rastall theory of gravity has been discussed in [49]. Gravity's rainbow [50] is a distortion of space-time which is an extension of the doubly special relativity for curved space-times. The properties of neutron stars and dynamical stability conditions in the modified TOV in gravity's rainbow have been investigated by Hendi et al [51]. The gravity's rainbow and compact star models have been studied in [52]. The rainbow's star models have also been studied in [53]. Recently, Mota et al [54] have studied the neutron star model in the framework of Rastall-Rainbow theories of gravity.

The main motivation of the work is to study the gravastar system in the framework of Rastall-Rainbow gravity with the isotropic fluid and electromagnetic source and examine the nature of physical parameters and stability of the gravastar. The organization of the work is as follows: In section II, we present the Rastall-Rainbow gravity theory with electromagnetic field. Here we write the Einstein-Maxwell field equations for spherically symmetric stellar metric in the framework of Rastall-Rainbow gravity. Section III deals with the geometry of gravastar and we compute the solutions in the three regions of gravastar model. In section IV, we analyze the physical aspects of the parameters of gravastar model. In section V, we investigate the matching between interior and exterior regions. Due to the junction conditions, we compute the equation of state, mass of the thin shell region and examine the stability of the gravastar. Finally some physical analysis and fruitful conclusions of the work are drawn in section VI.

## II. RASTALL-RAINBOW GRAVITY

In Einstein's General Relativity (GR), the conservation law of energy-momentum tensor is  $T_{\mu;\nu}^{\nu} = 0$ . The Rastall's Gravity is a generalization of General Relativity, where Rastall [45] proposed the modification of conservation law of energy-momentum tensor in curved space-time and which is given by [54]

$$T_{\mu;\nu}^{\nu} = \bar{\lambda}R_{,\mu} \quad (1)$$

where  $\bar{\lambda} = \frac{1-\lambda}{16\pi G}$  with  $\lambda$  is a constant called Rastall parameter, which measures the deviation from GR and describes the affinity of the matter field to couple with geometry. For  $\lambda = 1$ , the usual conservation law can be restored. Also for flat space-time, the Ricci scalar  $R = 0$  and we may also the usual conservation law. So for the effect of Rastall's gravity,  $\lambda \neq 1$  and the space-time must be non-flat. The

above equation can be written as

$$(T_{\mu}^{\nu} - \bar{\lambda}\delta_{\mu}^{\nu}R)_{;\nu} = 0 \quad (2)$$

So for Rastall's gravity, the Einstein's equation can be modified to the form

$$R_{\mu}^{\nu} - \frac{1}{2}\delta_{\mu}^{\nu}R = 8\pi G (T_{\mu}^{\nu} - \bar{\lambda}\delta_{\mu}^{\nu}R) \quad (3)$$

which can be simplified to the form

$$R_{\mu}^{\nu} - \frac{\lambda}{2}\delta_{\mu}^{\nu}R = 8\pi GT_{\mu}^{\nu} \quad (4)$$

Now the trace of the energy-momentum tensor is given by

$$T = \frac{(1-2\lambda)R}{8\pi G} \quad (5)$$

So the above Einstein's equation in Rastall's gravity can be written as

$$R_{\mu}^{\nu} - \frac{1}{2}\delta_{\mu}^{\nu}R = 8\pi G \left( T_{\mu}^{\nu} - \frac{(1-\lambda)}{2(1-2\lambda)}\delta_{\mu}^{\nu}T \right) \quad (6)$$

Now assume that the fluid source is composed of normal matter and electro-magnetic field. So the energy momentum tensor can be written as

$$T_{\mu\nu} = T_{\mu\nu}^M + T_{\mu\nu}^{EM} \quad (7)$$

where the energy-momentum tensor for normal matter is given by

$$T_{\mu\nu}^M = (\rho + p)u_{\mu}u_{\nu} + pg_{\mu\nu} \quad (8)$$

where  $u^{\mu}$  is the fluid four-velocity satisfying  $u_{\mu}u^{\mu} = -1$ ,  $\rho$  and  $p$  are the energy density and pressure of fluid. Further, the energy momentum tensor for electromagnetic field is given by [55]

$$T_{\mu\nu}^{EM} = -\frac{1}{4\pi}(g^{\delta\omega}F_{\mu\delta}F_{\omega\nu} - \frac{1}{4}g_{\mu\nu}F_{\delta\omega}F^{\delta\omega}) \quad (9)$$

where  $F_{\mu\nu}$  is the Maxwell field tensor defined as in the form:

$$F_{\mu\nu} = \Phi_{\nu,\mu} - \Phi_{\mu,\nu} \quad (10)$$

and  $\Phi_{\mu}$  is the four potential. The corresponding equations for Maxwell's electromagnetic field are given by

$$(\sqrt{-g}F^{\mu\nu})_{;\nu} = 4\pi J^{\mu}\sqrt{-g}, \quad F_{[\mu\nu,\delta]} = 0 \quad (11)$$

where  $J^{\mu}$  is the current four-vector satisfying  $J^{\mu} = \sigma u^{\mu}$ , the parameter  $\sigma$  is the charge density.

Magueijo and Smolin [50] have proposed gravity's Rainbow, which is an extension of the doubly special relativity for curved space-times. Gravity's rainbow is a distortion of space-time induced by two arbitrary functions  $\Pi(x)$  and  $\Sigma(x)$  (called the Rainbow functions) satisfying

$$\mathcal{E}^2\Pi^2(x) - v^2\Sigma^2(x) = m^2 \quad (12)$$

where  $x = \mathcal{E}/\mathcal{E}_{Pl}$ . Here  $\mathcal{E}$ ,  $v$ ,  $m$  and  $\mathcal{E}_{Pl} = \sqrt{\hbar c^5}/G$  are the energy, momentum, mass of a test particle and Planck energy respectively. Awad et al [56] and Khodadi et al [57] have chosen  $\Pi(x) = 1$  and  $\Sigma(x) = \sqrt{1+x^2}$  to study the solutions corresponding to a nonsingular universe. Also to study of gamma ray burst, the exponential form of rainbow has been applied in [56, 58]. In the absence of the test particles, the Rainbow functions are satisfying

$$\lim_{x \rightarrow 0} \Pi(x) = 1, \quad \lim_{x \rightarrow 0} \Sigma(x) = 1 \quad (13)$$

Mota et al [54] have merged the Rastall's gravity with Rainbow's gravity and applied the Rastall-Rainbow gravity theory in the neutron star formation. We consider the spherically symmetric metric describing the interior space-time of a star in Rainbow gravity as [54]

$$ds^2 = -\frac{B(r)}{\Pi^2(x)} dt^2 + \frac{A(r)}{\Sigma^2(x)} dr^2 + \frac{r^2}{\Sigma^2(x)} (d\theta^2 + \sin^2 \theta d\phi^2) \quad (14)$$

where  $A(r)$  and  $B(r)$  are functions of  $r$ . Since  $\Pi(x)$  and  $\Sigma(x)$  depend on  $x = \mathcal{E}/\mathcal{E}_{Pl}$  and  $\mathcal{E}$  is independent of  $r$ , so  $\Pi(x)$  and  $\Sigma(x)$  are independent of  $r$ . The metric coefficients depend of the energy of the test particle. So the geometry of the space-time becomes energy dependent. It should be noted that the metric coordinates do not depend on the energy of the particle.

For the charged fluid source with density  $\rho(r)$ , pressure  $p(r)$  and electromagnetic field  $E(r)$ , the Einstein-Maxwell (EM) equations in the Rastall-Rainbow gravity can be written in the form [54]

$$\frac{A'}{rA^2} - \frac{1}{r^2A} + \frac{1}{r^2} = 8\pi G\bar{\rho}, \quad (15)$$

$$\frac{B'}{rAB} + \frac{1}{r^2A} - \frac{1}{r^2} = 8\pi G\bar{p}_1, \quad (16)$$

and

$$\frac{B''}{2AB} - \frac{A'B'}{4A^2B} - \frac{B'^2}{4AB^2} - \frac{A'}{2rA^2} + \frac{B'}{2rAB} = 8\pi G\bar{p}_2 \quad (17)$$

where

$$\bar{\rho} = \frac{1}{\Sigma^2(x)} \left( \alpha_1 \rho + 3\alpha_2 p + \frac{1}{8\pi} (\alpha_1 - 3\alpha_2) E^2 \right), \quad (18)$$

$$\bar{p}_1 = \frac{1}{\Sigma^2(x)} \left( \alpha_2 \rho + (1 - 3\alpha_2) p + \frac{1}{8\pi} (4\alpha_2 - 1) E^2 \right), \quad (19)$$

and

$$\bar{p}_2 = \frac{1}{\Sigma^2(x)} \left( \alpha_2 \rho + (1 - 3\alpha_2) p + \frac{1}{8\pi} (1 - 2\alpha_2) E^2 \right) \quad (20)$$

with

$$\alpha_1 = \frac{3\lambda - 1}{2(2\lambda - 1)}, \quad \alpha_2 = \frac{\lambda - 1}{2(2\lambda - 1)} \quad (21)$$

We observe that  $\alpha_1 + \alpha_2 = 1$  and  $\lambda \neq 1/2$ . Adding equations (15) and (16), we obtain

$$\frac{1}{rA} \left( \frac{A'}{A} + \frac{B'}{B} \right) = 8\pi G(\bar{\rho} + \bar{p}_1) = \frac{8\pi G}{\Sigma^2(x)} (\rho + p) \quad (22)$$

From equation (15), we obtain [54]

$$A(r) = \left( 1 - \frac{2GM(r)}{r} \right)^{-1} \quad (23)$$

where the gravitational mass is

$$M(r) = \int_0^r 4\pi r'^2 \bar{\rho}(r') dr' \quad (24)$$

From the modification of conservation law of energy-momentum tensor, we obtain

$$p' + (\rho + p) \frac{B'}{2B} = \frac{1}{8\pi r^4} (r^4 E^2)' \quad (25)$$

and the electric field  $E$  is as follows

$$E(r) = \frac{1}{r^2} \int_0^r 4\pi r'^2 \sigma(r') \frac{\sqrt{A(r')}}{\Sigma(x)} dr' \quad (26)$$

The term  $\frac{\sigma\sqrt{A}}{\Sigma(x)}$  inside the above integral is known as the volume charge density.

### III. GRAVASTAR

Here, we will derive the solutions of the field equations for charged gravastar (charge is generated by electromagnetic field) and analyze its physical as well as geometrical interpretations. Since there are three regions of the gravastar, so the geometrical regions of the gravastar having a finite extremely thin width within the regions  $D = r_1 < r < r_2 = D + \epsilon$  where  $r_1$  and  $r_2$  are radii of the interior region and exterior region of the gravastar and  $\epsilon$  is very small positive quantity. The three regions are structured as follows: (i) *Interior region*  $R_1$ :  $0 \leq r < r_1$  with the equation of state (EOS) follows  $p = -\rho$ , (ii) *Shell region*  $R_2$ :  $r_1 < r < r_2$  with EOS follows  $p = \rho$  and (iii) *Exterior region*  $R_3$ :  $r_2 < r$  with EOS follows  $p = \rho = 0$ .

#### A. Interior Region

The interior region  $R_1$  ( $0 \leq r < r_1 = D$ ) of the gravastar follows the EoS  $p = -\rho$ . From equation (17), we obtain the relation

$$B(r) = kA^{-1}(r) \quad (27)$$

where  $k$  is constant  $> 0$ . There are 4 equations and 5 unknown functions  $A$ ,  $B$ ,  $\rho$ ,  $p$ ,  $E$  in the system. So one function is free to us. Here we may consider  $E$  is free function of  $r$  and is chosen by

$$E(r) = E_0 r^m \quad (28)$$

where  $m$  is positive constant and  $E_0$  is function of  $x$ .

Using equation (25), we obtain

$$p = -\rho = k_1 r^{2m} - k_2 \quad (29)$$

where  $k_1 = \frac{(m+2)E_0^2}{8\pi m}$  and  $k_2$  is positive constant. From (24), we obtain

$$M(r) = \frac{1}{2(2\lambda-1)\Sigma^2(x)} \left( \frac{8\pi k_2}{3} r^3 - \frac{2E_0^2}{m(2m+3)} r^{2m+3} \right) \quad (30)$$

From equation (23), we obtain the solution

$$B(r) = kA^{-1}(r) = k \left[ 1 - \frac{8\pi G k_2}{3(2\lambda-1)\Sigma^2(x)} r^2 + \frac{2GE_0^2}{m(2m+3)(2\lambda-1)\Sigma^2(x)} r^{2m+2} \right] \quad (31)$$

So the metric becomes (choose  $k = 1$ )

$$ds^2 = -\frac{1}{\Pi^2(x)} \left[ 1 - \frac{8\pi G k_2}{3(2\lambda-1)\Sigma^2(x)} r^2 + \frac{2GE_0^2}{m(2m+3)(2\lambda-1)\Sigma^2(x)} r^{2m+2} \right] dt^2 + \frac{1}{\Sigma^2(x)} \left[ 1 - \frac{8\pi G k_2}{3(2\lambda-1)\Sigma^2(x)} r^2 + \frac{2GE_0^2}{m(2m+3)(2\lambda-1)\Sigma^2(x)} r^{2m+2} \right]^{-1} dr^2 + \frac{r^2}{\Sigma^2(x)} (d\theta^2 + \sin^2 \theta d\phi^2) \quad (32)$$

The charge density for electric field is obtained in the form:

$$\sigma(r) = \frac{(m+2)E_0 r^{m-1}}{4\pi} \left[ 1 - \frac{8\pi G k_2}{3(2\lambda-1)\Sigma^2(x)} r^2 + \frac{2GE_0^2}{m(2m+3)(2\lambda-1)\Sigma^2(x)} r^{2m+2} \right]^{\frac{1}{2}} \quad (33)$$

Also the gravitational mass of the interior region of the charged gravastar can be found as

$$M(D) = \frac{1}{2(2\lambda-1)\Sigma^2(x)} \left( \frac{8\pi k_2}{3} D^3 - \frac{2E_0^2}{m(2m+3)} D^{2m+3} \right) \quad (34)$$

We observe that the quantities  $A(r)$ ,  $B(r)$ ,  $M(r)$ ,  $\sigma(r)$  depend on the Rastall parameter  $\lambda$  and Rainbow function  $\Sigma(x)$ .

## B. Shell Region

In the shell region  $R_2$  ( $D = r_1 < r < r_2 = D + \epsilon$ ), we assume that the thin shell region contains stiff perfect fluid which obeys EoS  $p = \rho$ . For this EoS, it is very difficult to obtain the solution from the field equations. So we shall assume the limit  $0 < A^{-1} \equiv h \ll 1$  in the thin shell to

obtain the analytical solution within the thin shell. Under this approximation (we can set  $h \approx 0$  to the leading order) with  $p = \rho$ , the field equations (15) - (17) reduce to the following forms

$$-\frac{h'}{r} + \frac{1}{r^2} = \frac{8\pi G}{\Sigma^2(x)} \left[ (\alpha_1 + 3\alpha_2)\rho + \frac{1}{8\pi} (\alpha_1 - 3\alpha_2)E^2 \right], \quad (35)$$

$$-\frac{1}{r^2} = \frac{8\pi G}{\Sigma^2(x)} \left[ (1 - 2\alpha_2)\rho + \frac{1}{8\pi} (4\alpha_2 - 1)E^2 \right] \quad (36)$$

and

$$\left( \frac{B'}{4B} + \frac{1}{2r} \right) h' = \frac{8\pi G}{\Sigma^2(x)} \left[ (1 - 2\alpha_2)\rho + \frac{1}{8\pi} (1 - 2\alpha_2)E^2 \right] \quad (37)$$

Eliminating  $\rho$  from the above equations, we ultimately get following two equations

$$-\frac{\lambda h'}{r} + \frac{2(2\lambda-1)}{r^2} = \frac{2G}{\Sigma^2(x)} E^2 \quad (38)$$

and

$$\left( \frac{B'}{4B} + \frac{1}{2r} \right) h' + \frac{1}{r^2} = \frac{(\lambda+1)G}{(2\lambda-1)\Sigma^2(x)} E^2 \quad (39)$$

We see that there are two equations but three unknowns  $B$ ,  $h$  and  $E$ . Similar to the assumption of interior region, let us assume that the solution of  $E$  is in the form  $E(r) = E_0 r^m$ . Solving equations (38) and (39), we obtain

$$A^{-1}(r) \equiv h(r) = h_1 + \frac{2(2\lambda-1)}{\lambda} \log r - \frac{E_0^2 G}{\lambda(m+1)\Sigma^2(x)} r^{2m+2} \quad (40)$$

and

$$B(r) = \frac{h_2}{r^2} \text{Exp} \left[ \int \frac{4\lambda[(\lambda+1)E_0^2 G r^{2m+2} - (2\lambda-1)\Sigma^2(x)] dr}{r(2\lambda-1)[2(2\lambda-1)\Sigma^2(x) - 2E_0^2 G r^{2m+2}]} \right] \quad (41)$$

where  $h_1$  and  $h_2$  are integration constants. In this shell region  $R_2$ , the range of  $r$  is satisfying  $D < r < D + \epsilon$ . Since  $h \ll 1$ , so  $\epsilon \ll 1$ . Under this assumption, we must have  $h_1 \ll 1$ . From equation (36) we obtain

$$p = \rho = \frac{E_0^2 r^{2m}}{8\pi\lambda} + \frac{(1-2\lambda)\Sigma^2(x)}{8\pi G \lambda r^2} \quad (42)$$

Also the charge density for electric field can be obtained in the form

$$\sigma(r) = \frac{(m+2)E_0 r^{m-1}}{4\pi} \left[ h_1 + \frac{2(2\lambda-1)}{\lambda} \log r - \frac{E_0^2 G}{\lambda(m+1)\Sigma^2(x)} r^{2m+2} \right]^{\frac{1}{2}} \quad (43)$$

We observe that the quantities  $A(r)$ ,  $B(r)$ ,  $\sigma(r)$ ,  $p$ ,  $\rho$  depend on the Rastall parameter  $\lambda$  and Rainbow function  $\Sigma(x)$ .

### C. Exterior Region

The exterior region  $R_3$  ( $r > r_2 = D + \epsilon$ ) contains the vacuum whose EoS is given by  $p = \rho = 0$ . In this exterior region, using equation (25), we obtain

$$E(r) = \frac{Q}{r^2} \quad (44)$$

where  $Q$  is constant electric charge. We obtain the solutions as

$$B(r) = kA^{-1}(r) = k \left( 1 - \frac{2GM}{r} + \frac{GQ^2}{(2\lambda - 1)\Sigma^2(x)r^2} \right) \quad (45)$$

where  $M$  is the mass of the charged gravastar.

So in the exterior region, the metric becomes (choose  $k = 1$ )

$$\begin{aligned} ds^2 = & -\frac{1}{\Pi^2(x)} \left( 1 - \frac{2GM}{r} + \frac{GQ^2}{(2\lambda - 1)\Sigma^2(x)r^2} \right) dt^2 \\ & + \frac{1}{\Sigma^2(x)} \left( 1 - \frac{2GM}{r} + \frac{GQ^2}{(2\lambda - 1)\Sigma^2(x)r^2} \right)^{-1} dr^2 \\ & + \frac{r^2}{\Sigma^2(x)} (d\theta^2 + \sin^2 \theta d\phi^2) \end{aligned} \quad (46)$$

which generates the Reissner-Nordstrom black hole in Rainbow gravity [59]. For  $Q = 0$ , the above metric reduces to the Schwarzschild black hole in Rainbow gravity [60]. Also we observe that the quantities  $A(r)$ ,  $B(r)$  depend on the Rastall parameter  $\lambda$  and Rainbow function  $\Sigma(x)$ .

## IV. PHYSICAL ASPECTS OF PARAMETERS OF CHARGED GRAVASTAR

Now we study the aspects of the physical parameters of the charged gravastar like proper length of the shell, energy and entropy within the shell. We shall also examine the impact of electromagnetic field on different physical features of the charged gravastar in the framework of Rastall-Rainbow gravity.

### A. Proper Length of the Thin Shell

Since the radius of inner boundary of the shell of the gravastar is  $r = D$  and the radius of outer boundary of the shell is  $r = D + \epsilon$ , where  $\epsilon$  is the proper thickness of the shell which is assumed to be very small (i.e.,  $\epsilon \ll 1$ ). So the stiff perfect fluid propagates between two boundaries of the thin shell region of the gravastar. Now, the proper length of the shell is described by [1]

$$\ell = \int_D^{D+\epsilon} \sqrt{\frac{A(r)}{\Sigma^2(x)}} dr \quad (47)$$

Since in the shell region, the expressions of  $A(r)$  is complicated, so it is very difficult to obtain the analytical form

of the above integral. So let us assume  $\sqrt{A(r)} = \frac{dg(r)}{dr}$ , so from the above integral we can write

$$\begin{aligned} \ell &= \frac{1}{\Sigma(x)} \int_D^{D+\epsilon} \frac{dg(r)}{dr} dr = \frac{1}{\Sigma(x)} [g(D + \epsilon) - g(D)] \\ &\approx \frac{\epsilon}{\Sigma(x)} \frac{dg(r)}{dr} \Big|_D = \frac{\epsilon \sqrt{A(D)}}{\Sigma(x)} \end{aligned} \quad (48)$$

since  $\epsilon \ll 1$ , so  $O(\epsilon^2) \approx 0$ . So in the above manipulation, we have considered only the first order term of  $\epsilon$ . Thus for this approximation, the proper length will be

$$\ell = \frac{\epsilon}{\Sigma(x)} \left[ h_1 + \frac{2(2\lambda - 1)}{\lambda} \log D - \frac{E_0^2 G}{\lambda(m+1)\Sigma^2(x)} D^{2m+2} \right]^{-\frac{1}{2}} \quad (49)$$

The above result shows that the proper length of the thin shell of the gravastar is proportional to the thickness  $\epsilon$  of the shell. We observe that proper length of the thin shell depends on the electric field  $E_0$  of the gravastar, Rastall parameter  $\lambda$  and Rainbow function  $\Sigma(x)$ . Due to Awad et al [56] and Khodadi et al [57], here we have chosen  $\Sigma(x) = \sqrt{1+x^2}$  where  $x = \mathcal{E}/\mathcal{E}_{Pl}$ . We have plotted the proper length  $\ell$  vs thickness  $\epsilon$  and radius  $D$  in fig. 1 and fig.2 respectively. From the figures, we have seen that the proper length  $\ell$  increases with the thickness  $\epsilon$  of the shell of the charged gravastar but decreases as radius  $D$  increases. On the other hand, we have also plotted the proper length  $\ell$  vs Rastall parameter  $\lambda$  and test particle's charge  $\mathcal{E}$  in fig. 3. From the figure, we have observed that the proper length  $\ell$  very slowly decreases as Rastall parameter  $\lambda$  increases and smoothly decreases as the test particle's charge  $\mathcal{E}$  increases.

### B. Energy of the Charged Gravastar

The energy content within the shell region of the charged gravastar is given as [12]

$$\begin{aligned} \mathcal{W} &= \int_D^{D+\epsilon} 4\pi r^2 \bar{\rho} dr \\ &= \frac{1}{2\lambda G \Sigma^2(x)} \left[ \frac{2GE_0^2}{2m+3} ((D+\epsilon)^{2m+3} - D^{2m+3}) \right. \\ &\quad \left. - \epsilon(3\lambda - 2)\Sigma^2(x) \right] \end{aligned} \quad (50)$$

For the approximation  $\epsilon \ll 1$  due to thin shell region of the gravastar, we may obtain

$$\mathcal{W} = \frac{\epsilon}{2\lambda G \Sigma^2(x)} [2GE_0^2 D^{2m+2} - (3\lambda - 2)\Sigma^2(x)] \quad (51)$$

We see that the energy content in the shell is proportional to the thickness ( $\epsilon$ ) of the shell. Also we observe that the energy of the gravastar depends on the electric field  $E_0$  of the gravastar, Rastall parameter  $\lambda$  and Rainbow function  $\Sigma(x)$ . We have plotted the energy content  $\mathcal{W}$  in the shell vs thickness  $\epsilon$  and radius  $D$  in fig. 4 and fig.5 respectively. From the figures, we have seen that the the energy content  $\mathcal{W}$  in the shell increases with the thickness  $\epsilon$  of the shell

of the charged gravastar as well as the radius  $D$ . On the other hand, we have also plotted the energy content  $\mathcal{W}$  in the shell vs Rastall parameter  $\lambda$  and test particle's charge  $\mathcal{E}$  in fig. 6. From the figure, we have observed that the energy content  $\mathcal{W}$  in the shell decreases as increase of the Rastall content  $\lambda$  and the test particle's charge  $\mathcal{E}$ .

### C. Entropy of the Charged Gravastar

Entropy is the disorderness within the body of a gravastar. Mazur and Mottola [1, 2] have shown that the entropy density in the interior region  $R_1$  of the gravastar is zero. But, the entropy within the thin shell can be described by [1]

$$\mathcal{S} = \int_D^{D+\epsilon} 4\pi r^2 s(r) \sqrt{\frac{A(r)}{\Sigma^2(x)}} dr \quad (52)$$

where  $s(r)$  is the entropy density corresponding to the specific temperature  $T(r)$  and which can be defined as

$$s(r) = \frac{\gamma^2 k_B^2 T(r)}{4\pi\hbar} = \frac{\gamma k_B}{\hbar} \sqrt{\frac{p(r)}{2\pi}} \quad (53)$$

where  $\gamma$  is dimensionless constant. So entropy within the thin shell can be written as

$$\begin{aligned} \mathcal{S} &= \frac{\gamma k_B}{\hbar \Sigma(x)} \int_D^{D+\epsilon} r^2 \sqrt{8\pi p(r) A(r)} dr \\ &= \frac{\gamma k_B}{\hbar \sqrt{\lambda G} \Sigma(x)} \int_D^{D+\epsilon} r [GE_0^2 r^{2m+2} + (1-2\lambda)\Sigma^2(x)]^{\frac{1}{2}} \times \\ &\quad \left[ h_1 + \frac{2(2\lambda-1)}{\lambda} \log r - \frac{E_0^2 G}{\lambda(m+1)\Sigma^2(x)} r^{2m+2} \right]^{-\frac{1}{2}} dr \end{aligned} \quad (54)$$

Now it is very difficult to obtain analytical form of the above integral. So using the approximation  $\epsilon \ll 1$ , we can obtain

$$\begin{aligned} \mathcal{S} &\approx \frac{\epsilon \gamma k_B}{\hbar \Sigma(x)} D^2 \sqrt{8\pi p(D) A(D)} \\ &\approx \frac{\epsilon \gamma k_B D}{\hbar \sqrt{\lambda G} \Sigma(x)} [GE_0^2 D^{2m+2} + (1-2\lambda)\Sigma^2(x)]^{\frac{1}{2}} \times \\ &\quad \left[ h_1 + \frac{2(2\lambda-1)}{\lambda} \log D - \frac{E_0^2 G}{\lambda(m+1)\Sigma^2(x)} D^{2m+2} \right]^{-\frac{1}{2}} \end{aligned} \quad (55)$$

This result shows that the entropy in the shell of the charged gravastar is proportional to the thickness  $\epsilon$  of the shell. We observe that the entropy depends on the electric field  $E_0$  of the gravastar, Rastall parameter  $\lambda$  and Rainbow function  $\Sigma(x)$ . We have plotted the entropy  $\mathcal{S}$  within the shell vs thickness  $\epsilon$  and radius  $D$  in fig. 7 and fig.8 respectively. From the figures, we have seen that the the entropy  $\mathcal{S}$  within the shell increases with the thickness  $\epsilon$  of the shell of the charged gravastar as well as the radius

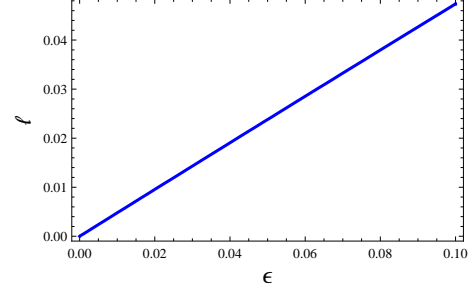


Fig. 1 represents the plot proper length  $\ell$  vs thickness  $\epsilon$ .

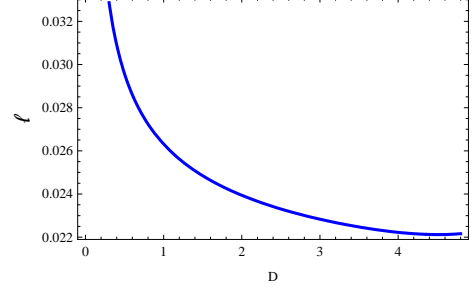


Fig. 2 represents the plot of proper length  $\ell$  vs radius  $D$ .

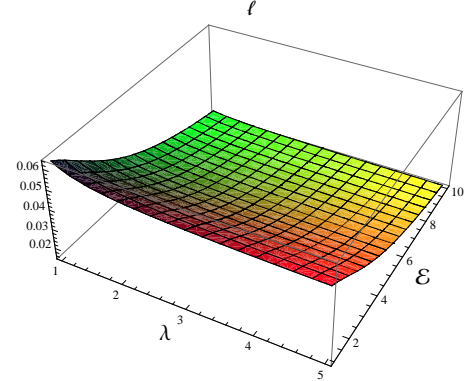


Fig. 3 represents the plot of proper length  $\ell$  vs Rastall parameter  $\lambda$  and test particle's charge  $\mathcal{E}$ .

$D$ . On the other hand, we have also plotted the entropy  $\mathcal{S}$  within the shell vs Rastall parameter  $\lambda$  and test particle's charge  $\mathcal{E}$  in fig. 9. From the figure, we have observed that the entropy  $\mathcal{S}$  within the shell decreases as increase of the Rastall parameter  $\lambda$  and the test particle's charge  $\mathcal{E}$ .

## V. JUNCTION CONDITIONS BETWEEN INTERIOR AND EXTERIOR REGIONS

Since gravastar consists of three regions: interior region, thin shell region and exterior region, so according to the Darmois-Israel formalism [61–63] we want to study the matching between the surfaces of the interior and exterior regions. We denote  $\Sigma$  is the junction surface which is located at  $r = D$ . In the Rainbow gravity, we consider the

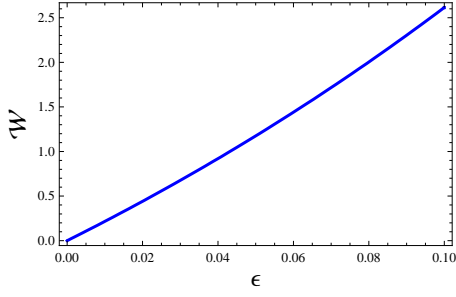


Fig. 4 represents the plot of energy content  $\mathcal{W}$  vs thickness  $\epsilon$ .

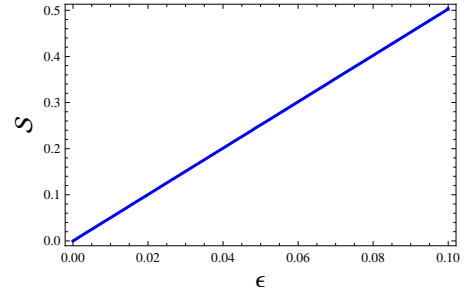


Fig. 7 represents the plot of entropy  $\mathcal{S}$  vs thickness  $\epsilon$ .

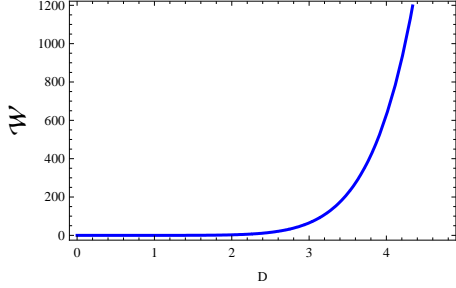


Fig. 5 represents the plot of energy content  $\mathcal{W}$  vs radius  $D$ .

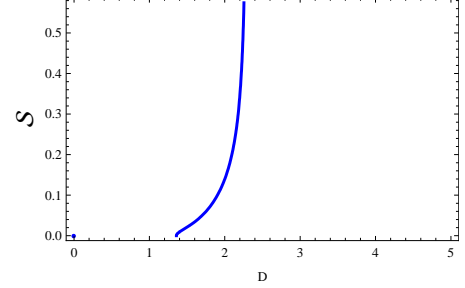


Fig. 8 represents the plot of entropy  $\mathcal{S}$  vs radius  $D$ .

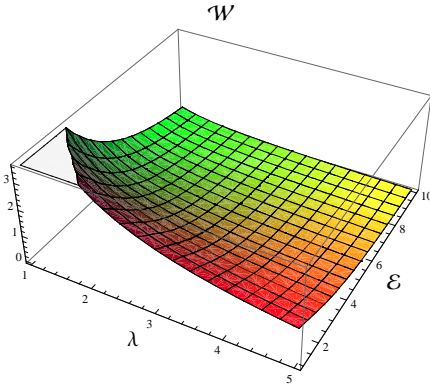


Fig. 6 represents the plot of energy content  $\mathcal{W}$  vs Rastall parameter  $\lambda$  and test particle's charge  $\mathcal{E}$ .

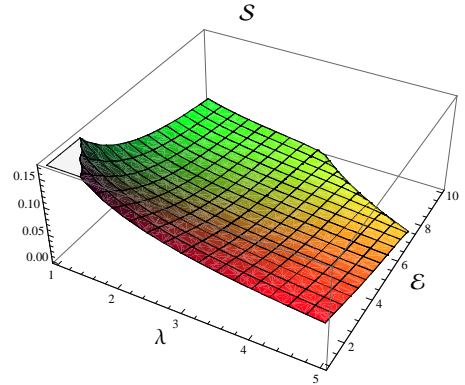


Fig. 9 represents the plot of entropy  $\mathcal{S}$  vs Rastall parameter  $\lambda$  and test particle's charge  $\mathcal{E}$ .

metric on the junction surface as in the form

$$ds^2 = -\frac{f(r)}{\Pi^2(x)} dt^2 + \frac{1}{\Sigma^2(x)f(r)} dr^2 + \frac{r^2}{\Sigma^2(x)} (d\theta^2 + \sin^2 \theta d\phi^2) \quad (56)$$

where the metric coefficients are continuous at the junction surface  $\Sigma$ , but their derivatives might not be continuous at  $\Sigma$ . In the joining surface  $S$ , the surface tension and surface stress energy may be resolved by the discontinuity of the extrinsic curvature of  $S$  at  $r = D$ . The expression of the stress-energy surface  $S_{ij}$  is defined by the Lanczos equation [64] (with the help of Darmois-Israel formalism)

$$S_j^i = -\frac{1}{8\pi} (\eta_j^i - \delta_j^i \eta_k^k) \quad (57)$$

where  $\eta_{ij} = K_{ij}^+ - K_{ij}^-$ . Here  $K_{ij}$  denotes the extrinsic curvature. Here the signs “-” and “+” respectively correspond to the interior and the exterior regions of the gravastar. So  $\eta_{ij}$  describes the discontinuous surfaces in the second fundamental forms of the extrinsic curvatures.

The extrinsic curvatures on the both surfaces of the shell region can be described by

$$K_{ij}^\pm = \left[ -n_\nu^\pm \left\{ \frac{\partial^2 x_\nu}{\partial \xi^i \partial \xi^j} + \Gamma_{\alpha\beta}^\nu \frac{\partial x^\alpha}{\partial \xi^i} \frac{\partial x^\beta}{\partial \xi^j} \right\} \right]_\Sigma \quad (58)$$

where  $\xi^i$  represent the intrinsic coordinates on the shell,  $n_\nu^\pm$  describe the unit normals to the surface  $\Sigma$  of the gravastar, defined by  $n_\nu n^\nu = -1$ . For the above metric, we can obtain

$$n_\nu^\pm = \pm \left[ g^{\alpha\beta} \frac{\partial f}{\partial x^\alpha} \frac{\partial f}{\partial x^\beta} \right]^{-\frac{1}{2}} \frac{\partial f}{\partial x^\nu} \quad (59)$$

According to the Lanczos equation, the stress-energy surface tensor can be written as  $S_j^i = \text{diag}(-\varrho, \mathcal{P}, \mathcal{P}, \mathcal{P})$  where  $\varrho$  is the surface energy density and  $\mathcal{P}$  is the surface pressure. Using the matching conditions, in the charged gravastar model, the surface energy density and the surface pressure can be obtained as

$$\varrho(D) = \frac{1}{4\pi D} (1 - q_2(x)D^2 + q_3(x)D^{2m+2})^{\frac{1}{2}}$$

$$-\frac{1}{4\pi D} \left(1 - \frac{2GM}{D} + \frac{q_1(x)}{D^2}\right)^{\frac{1}{2}} \quad (60)$$

and

$$\begin{aligned} \mathcal{P}(D) &= \frac{1}{8\pi D} \left(1 - \frac{2GM}{D} + \frac{q_1(x)}{D^2}\right)^{\frac{1}{2}} \\ &- \frac{1}{8\pi D} (1 - q_2(x)D^2 + q_3(x)D^{2m+2})^{\frac{1}{2}} \\ &+ \frac{1}{16\pi} \left(\frac{GM}{D^2} - \frac{q_1(x)}{D^3}\right) \left(1 - \frac{2GM}{D} + \frac{q_1(x)}{D^2}\right)^{-\frac{1}{2}} \\ &- \frac{1}{16\pi} (-q_2(x)D + (m+1)q_3(x)D^{2m+1}) \times \\ &(1 - q_2(x)D^2 + q_3(x)D^{2m+2})^{-\frac{1}{2}} \end{aligned} \quad (61)$$

where

$$\begin{aligned} q_1(x) &= \frac{GQ^2}{(2\lambda - 1)\Sigma^2(x)}, \quad q_2(x) = \frac{8\pi Gk_2}{3(2\lambda - 1)\Sigma^2(x)}, \\ q_3(x) &= \frac{2G}{m(2m+3)(2\lambda - 1)\Sigma^2(x)}. \end{aligned} \quad (62)$$

We have drawn the plots of surface energy density  $\varrho(D)$  and surface pressure  $\mathcal{P}(D)$  vs radius  $D$  in fig. 10 and fig. 12. From these figures we have seen that the surface energy density  $\varrho(D)$  increases and surface pressure  $\mathcal{P}(D)$  decreases as radius  $D$  increases. On the other hand, we have drawn the plots of surface energy density  $\varrho(D)$  and surface pressure  $\mathcal{P}(D)$  vs Rastall parameter  $\lambda$  and test particle's charge  $\mathcal{E}$  in fig. 11 and fig. 13. We have observed that if Rastall parameter  $\lambda$  and test particle's charge  $\mathcal{E}$  increase then surface energy density  $\varrho(D)$  decreases but surface pressure  $\mathcal{P}(D)$  increases. Also we have seen that surface pressure  $\mathcal{P}(D)$  is always keep negative sign.

### A. Equation of State

The equation of state parameter  $w(D)$  (at  $r = D$ ) can be described as

$$w(D) = \frac{\mathcal{P}(D)}{\varrho(D)} \quad (63)$$

So the equation of state parameter can be obtained in the following form

$$\begin{aligned} w(D) &= -\frac{1}{2} + \frac{1}{4} \left[ \left( \frac{GM}{D^2} - \frac{q_1(x)}{D^3} \right) \times \right. \\ &\left. \left( 1 - \frac{2GM}{D} + \frac{q_1(x)}{D^2} \right)^{-\frac{1}{2}} \right. \\ &- (-q_2(x)D + (m+1)q_3(x)D^{2m+1}) \times \\ &\left. \left. \left( 1 - q_2(x)D^2 + q_3(x)D^{2m+2} \right)^{-\frac{1}{2}} \right] \times \right. \\ &\left. \left[ \left( 1 - q_2(x)D^2 + q_3(x)D^{2m+2} \right)^{\frac{1}{2}} \right. \right. \\ &\left. \left. - \left( 1 - \frac{2GM}{D} + \frac{q_1(x)}{D^2} \right)^{\frac{1}{2}} \right]^{-1} \end{aligned} \quad (64)$$

We have plotted the equation of state parameter  $w(D)$  vs radius  $D$  in fig. 14 and seen that  $w(D)$  increases as radius  $D$  increases. Also we have plotted the equation of state parameter  $w(D)$  vs Rastall parameter  $\lambda$  and test particle's charge  $\mathcal{E}$  in fig. 15 and it decreases as Rastall parameter  $\lambda$  and test particle's charge  $\mathcal{E}$  increase but  $w(D)$  is always keep negative sign.

### B. Mass

The mass  $\mathcal{M}$  of the thin shell of the charged gravastar can be obtained from the following formula

$$\mathcal{M} = 4\pi D^2 \varrho(D) \quad (65)$$

which can be expressed as in the form

$$\begin{aligned} \mathcal{M} &= D \left[ \left( 1 - q_2(x)D^2 + q_3(x)D^{2m+2} \right)^{\frac{1}{2}} \right. \\ &\left. - \left( 1 - \frac{2GM}{D} + \frac{q_1(x)}{D^2} \right)^{\frac{1}{2}} \right] \end{aligned} \quad (66)$$

So the total mass  $M$  of the charged gravastar in terms of the mass of the thin shell can be expressed as

$$\begin{aligned} M &= \frac{D}{2G} + \frac{q_1(x)}{2GD} \\ &- \frac{D}{2G} \left[ \left( 1 - q_2(x)D^2 + q_3(x)D^{2m+2} \right)^{\frac{1}{2}} - \frac{\mathcal{M}}{D} \right]^2 \end{aligned} \quad (67)$$

We see that the total mass  $M$  of the gravastar will be less than  $\frac{D^2 + q_1(x)}{2GD}$ . We have plotted the mass  $\mathcal{M}$  of the thin shell of the charged gravastar vs radius  $D$  in fig. 16 and seen that the mass  $\mathcal{M}$  increases as radius  $D$  increases. Also we have plotted the the mass  $\mathcal{M}$  vs Rastall parameter  $\lambda$  and test particle's charge  $\mathcal{E}$  in fig. 17 and it decreases as Rastall parameter  $\lambda$  and test particle's charge  $\mathcal{E}$  increase.

### C. Stability

Poisson et al [65] have examined the linearized stability for thin shell wormhole. Lobo et al [66] have examined the linearized stability for thin shell wormhole with cosmological constant. Ovgun et al [28] have examined the stability of charged thin-shell gravastar. Also Yousaf et al [43] have discussed the stability of the gravastar in  $f(R, \mathcal{T})$  gravity. Motivated by their work, we want to analyze the stability of the charged gravastar in Rastall-Rainbow gravity. For this purpose, define a parameter  $\eta$  as follows [65]:

$$\eta(D) = \frac{\mathcal{P}'(D)}{\varrho'(D)} \quad (68)$$

The parameter  $\eta$  is interpreted as the squared speed of sound satisfying  $0 \leq \eta \leq 1$  normally. But for the stability of the gravastar, the restriction may not be satisfied on the surface layer. We have plotted  $\eta$  vs radius  $D$  in fig. 18 and seen that  $\eta$  decreases as radius  $D$  increases. Also we



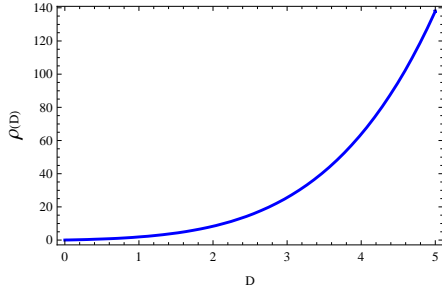


Fig. 10 represents the plot of surface energy density  $\varrho(D)$  vs radius  $D$ .

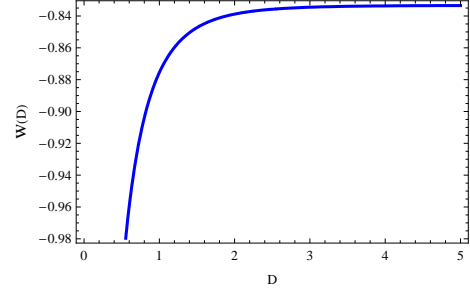


Fig. 14 represents the plot of equation of state parameter  $w(D)$  vs radius  $D$ .

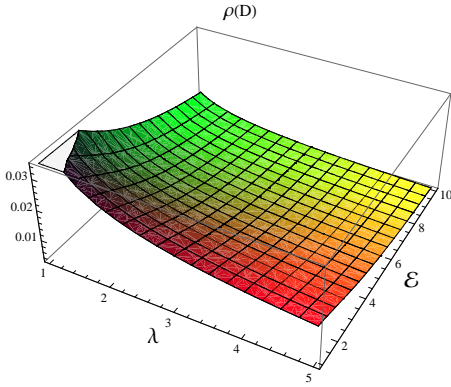


Fig. 11 represents the plot of surface energy density  $\varrho(D)$  vs Rastall parameter  $\lambda$  and test particle's charge  $\mathcal{E}$ .

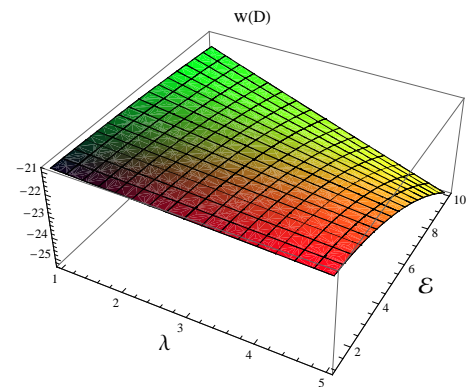


Fig. 15 represents the plot of equation of state parameter  $w(D)$  vs Rastall parameter  $\lambda$  and test particle's charge  $\mathcal{E}$ .

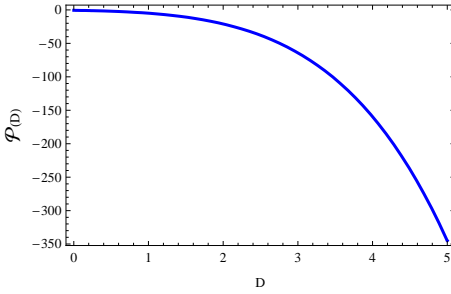


Fig. 12 represents the plot of surface pressure  $\mathcal{P}(D)$  vs radius  $D$ .

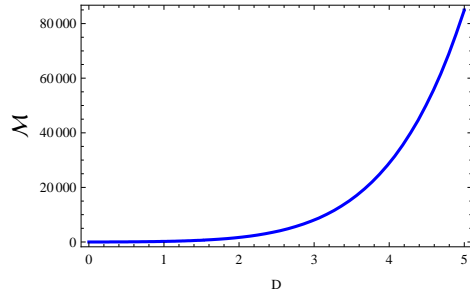


Fig. 16 represents the plot of the mass of the thin shell  $\mathcal{M}$  vs radius  $D$ .

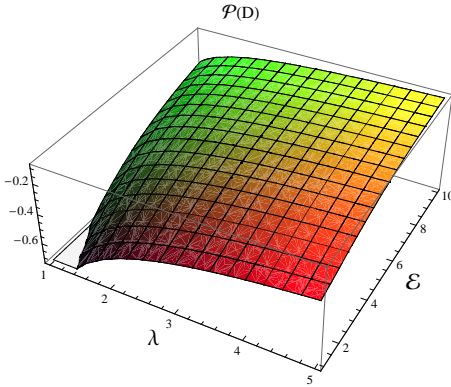


Fig. 13 represents the plot of surface pressure  $\mathcal{P}(D)$  vs Rastall parameter  $\lambda$  and test particle's charge  $\mathcal{E}$ .

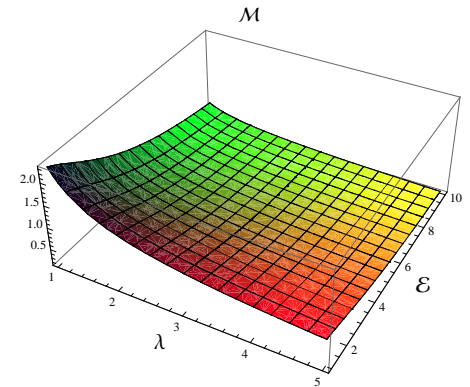


Fig. 17 represents the plot of the mass of the thin shell  $\mathcal{M}$  vs Rastall parameter  $\lambda$  and test particle's charge  $\mathcal{E}$ .

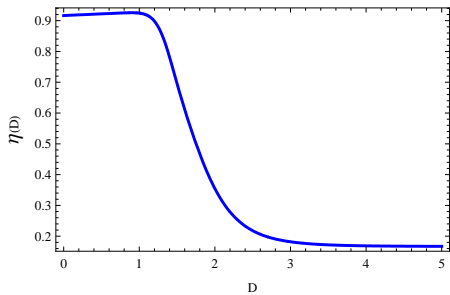


Fig. 18 represents the plot of  $\eta(D)$  vs radius  $D$ .

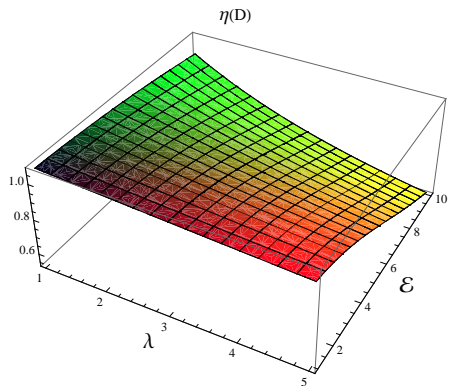


Fig. 19 represents the plot of  $\eta(D)$  vs Rastall parameter  $\lambda$  and test particle's charge  $\mathcal{E}$ .

have plotted  $\eta$  vs Rastall parameter  $\lambda$  and test particle's charge  $\mathcal{E}$  in fig. 19 and it decreases as Rastall parameter  $\lambda$  and test particle's charge  $\mathcal{E}$  increase. Figures show that  $\eta$  always keep positive sign which allows the stability of the gravastar model.

## VI. DISCUSSIONS

In this work, we have considered the spherically symmetric stellar system in the contexts of Rastall-Rainbow gravity theory in presence of isotropic fluid source with electro-magnetic field. The Einstein-Maxwell's field equations have been written in the framework of Rastall-Rainbow gravity. Next we have discussed the geometry of charged gravastar model. The gravastar consists of three regions: interior region, thin shell region and exterior region. In the interior region, the gravastar follows the equation of state (EoS)  $p = -\rho$  and we have found the solutions of all physical quantities like energy density, pressure, electric field, charge density, gravitational mass and metric coefficients. In the exterior region, we have obtained the exterior Riessner-Nordstrom solution for

vacuum model ( $p = \rho = 0$ ). In the shell region, the fluid source follows the EoS  $p = \rho$  (ultra-stiff perfect fluid). In this region, since we have assumed that the interior and exterior regions join together at a place, so the intermediate region must be thin shell and the thickness of the shell of the gravastar is infinitesimal. So the thin shell follows with the limit  $h (\equiv A^{-1}) \ll 1$ . Under this approximation, we have found the analytical solutions within the thin shell of the gravastar. The physical quantities like the proper length of the thin shell, energy content and entropy inside the thin shell of the charged gravastar have been computed and we have shown that they are directly proportional to the proper thickness of the shell ( $\epsilon$ ) due to the approximation ( $\epsilon \ll 1$ ). These physical quantities significantly depend on the Rastall parameter  $\lambda$  and Rainbow function  $\Sigma(x)$  (which depends on energy of the test particle). From figures 1 - 9, we have seen that the proper length of the thin shell, energy content and entropy inside the thin shell of the charged gravastar increase as thickness increases. Also the proper length decreases as radius increases. The energy content and entropy inside the thin shell always increase as radius increases. Moreover, if Rastall parameter  $\lambda$  and test particle's charge  $\mathcal{E}$  both increase then the proper length of the thin shell, energy content and entropy inside the thin shell all decrease. According to the Darmois-Israel formalism, we have studied the matching between the surfaces of interior and exterior regions of the charged gravastar and using the matching conditions, the surface energy density and the surface pressure have been obtained. Also the equation of state parameter on the surface, mass of the thin shell have been obtained and the total mass of the charged gravastar have been expressed in terms of the thin shell mass. From figures 10, 14, 16 we have observed that the surface density, equation of state and mass of the thin shell increase as radius increases but from figure 12, we have seen that the surface pressure always decreases as radius increases but keeps negative sign and hence the equation of state keeps negative sign. Also the figures 11, 15, 17 show that the surface density, equation of state and mass of the thin shell decrease as the increase of both Rastall parameter  $\lambda$  and test particle's charge  $\mathcal{E}$ . But figure 13 shows the surface pressure increases as the increase of both Rastall parameter  $\lambda$  and test particle's charge  $\mathcal{E}$ . Finally, we have explored the stable regions of the charged gravastar in Rastall-Rainbow gravity in figures 18 and 19. The figures show that  $\eta$  always decreases but keeps in positive sign as the increase of radius, Rastall parameter  $\lambda$  and test particle's charge  $\mathcal{E}$ .

- 
- [1] P. Mazur and E. Mottola, Report number: LA-UR-01- 5067 (arXiv:gr-qc/0109035).  
[2] P. Mazur and E. Mottola, Proc. Natl. Acad. Sci. (USA) 101, 9545 (2004).  
[3] M. Visser and D. L. Wiltshire, Class. Quant. Grav. 21, 1135

- (2004).  
[4] A. DeBenedictis, D. Horvat, S. Ilijic, S. Kloster and K. S. Viswanathan, Class. Quant. Grav. 23, 2303 (2006).  
[5] C. Cattoen, T. Faber and M. Visser, Class. Quant. Grav. 22, 4189 (2005).

- [6] N. Bilic, G. B. Tupper and R. D. Viollier, *JCAP* 0602, 013 (2006).
- [7] B. M. N. Carter, *Class. Quant. Grav.* 22, 4551 (2005).
- [8] A. A. Usmani, F. Rahaman, S. A. Rakib, S. Ray, K. K. Nandi, P. K. F. Kuhfittig and Z. Hasan, *Phys. Lett. B* 701, 388 (2011).
- [9] P. Bhar, *Astrophys. Space Sci.* 354, 2109 (2014).
- [10] A. Banerjee, F. Rahaman, S. Islam and M. Govender, *Eur. Phys. J. C* 76, 34 (2016).
- [11] F. Rahaman, S. Chakraborty, S. Ray, A. A. Usmani and S. Islam, *Int. J. Theor. Phys.* 54, 50 (2015).
- [12] S. Ghosh, F. Rahaman, B. K. Guha and S. Ray, *Phys. Lett. B* 767, 380 (2017).
- [13] S. Ghosh, S. Ray, F. Rahaman and B. K. Guha, *Annals of Phys.* 394, 230 (2018).
- [14] B. M. N. Carter, *Class. Quant. Grav.* 22, 4551 (2005).
- [15] P. Rocha, R. Chan, M. F. A. da Silva and A. Wang, *JCAP* 0811, 010 (2008).
- [16] P. Rocha, A. Y. Miguelote, R. Chan, M. F. da Silva, N. O. Santos and A. Wang, *JCAP* 0806, 025 (2008).
- [17] R. Chan, M. F. A. da Silva, P. Rocha and A. Wang, *JCAP* 0903, 010 (2009).
- [18] F. Rahaman, S. Ray, A. A. Usmani, Islam and S. Islam, *Phys. Lett. B* 707, 319 (2012).
- [19] F. S. N. Lobo and R. Garattini, *JHEP* 1312, 065 (2013).
- [20] A. Banerjee, J. R. Villanueva, P. Channuie and K. Jusuf, *Chin. Phys. C* 42, 115101 (2018).
- [21] F. de Felice, Y. Yu and J. Fang, *Mon. Not. R. Astron. Soc.* 277, L17 (1995).
- [22] B. V. Turimov, B. J. Ahmedov and A. A. Abdujabbarov, *Mod. Phys. Lett. A* 24, 733 (2009).
- [23] D. Horvat, S. Ilijic and A. Marunovic, *Class. Quant. Grav.* 26, 025003 (2009).
- [24] R. Chan and M. F. A. da Silva, *JCAP* 1007, 029 (2010).
- [25] F. Rahaman, A. A. Usmani, S. Ray and S. Islam, *Phys. Lett. B* 717, 1 (2012).
- [26] C. F. C. Brandt, R. Chan, M. F. A. da Silva and P. Rocha, *J. Mod. Phys.* 6, 879 (2013).
- [27] Z. Yousaf and M. Z. Bhatti, *Mon. Not. R. Astron. Soc.* 458, 1785 (2016).
- [28] A. Ovgun, A. Banerjee and K. Jusufi, *Eur. Phys. J. C* 77, 566 (2017).
- [29] S. Ray and B. Das, *Gravit. Cosmol.* 13, 224 (2007).
- [30] C. G. Boehmer, A. Mussa and N. Tamanini, *Class. Quant. Grav.* 28, 245020 (2011).
- [31] C. Deliduman and B. Yapiskan, arXiv:1103.2225 [gr-qc].
- [32] G. Abbas, S. Qaisar and M. A. Meraj, *Astrophys. Space Sci.* 357, 156 (2015).
- [33] P. Saha and U. Debnath, *Adv. High Energy Phys.* 2018, 3901790 (2018).
- [34] A. V. Kpadonou, M. J. S. Houndj and M. E. Rodrigues, *Astrophys. Space Sci.* 361, 244 (2016).
- [35] G. Abbas, S. Qaisar, W. Javed and M.A. Meraj, *Iran. J. Sci. Technol. A* 42, 1659 (2016).
- [36] M. G. Ganiou, C. Anamon, M. J. S. Houndjo and J. Tossa, *Eur. Phys. J. Plus* 132, 250 (2017).
- [37] K. D. Krori and J. Barua, *J. Phys. A: Math. Gen.* 8, 508 (1975).
- [38] G. Abbas, S. Nazeer and M. A. Meraj, *Astrophys. Space Sci.* 354, 449 (2014).
- [39] G. Abbas, A. Kanwal and M. Zubair, *Astrophys. Space Sci.* 357, 109 (2015).
- [40] G. Abbas et al, *Astrophys. Space Sci.* 357, 158 (2015).
- [41] G. Abbas, M. Zubair and G. Mustafa, *Astrophys. Space Sci.* 358, 26 (2015).
- [42] A. Das, S. Ghosh, B. K. Guha, S. Das, F. Rahaman and S. Ray, *Phys. Rev. D* 95, 124011 (2017).
- [43] Z. Yousaf, K. Bamba, M. Z. Bhatti and U. Ghafoor, *Phys. Rev. D* 100, 024062 (2019).
- [44] M. F. Shamir and M. Ahmad, *Phys. Rev. D* 97, 104031 (2018).
- [45] P. Rastall, *Phys. Rev. D* 6, 3357 (1972).
- [46] A. M. Oliveira, H. E. S. Velten, J. C. Fabris and L. Casarini, *Phys. Rev. D* 92, 044020 (2015).
- [47] G. Abbas and M. R. Shahzad, *Eur. Phys. J. A* 54, 211 (2018).
- [48] G. Abbas and M. R. Shahzad, *Astrophys. Space Sci.* 363, 251 (2018).
- [49] G. Abbas and M. R. Shahzad, *Astrophys. Space Sci.* 364, 50 (2019).
- [50] J. Magueijo and L. Smolin, *Class. Quantum Grav.* 21, 1725 (2004).
- [51] S. H. Hendi, G. H. Bordbar, B. E. Panah, S. Panahiyan, *JCAP* 1609, 013 (2016).
- [52] R. Garattini and G. Mandanici., arXiv:1601.00879 [physics.gen-ph].
- [53] R. Garattini and G. Mandanici, *Eur. Phys. J. C* 77, 57 (2017).
- [54] C. E. Mota, L. C. N. Santos, G. Grams, F. M. da Silva and D. P. Menezes, *Phys. Rev. D* 100, 024043 (2019).
- [55] U. Debnath, *Eur. Phys. J. C* 79, 499 (2019).
- [56] A. Awad, A. F. Ali and B. Majumder, *JCAP* 1310, 052 (2013).
- [57] M. Khodadi, K. Nozari and H. R. Sepangi, *Gen. Relativ. Grav.* 48, 166 (2016).
- [58] G. Amelino-Camelia et al, *Nature* 393, 763 (1998).
- [59] A. Haldar and R. Biswas, *Gen. Rel. Grav.* 51, 72 (2019).
- [60] C. Leiva, J. Saavedra and J. Villanueva, *Mod. Phys. Lett. A* 24, 1443 (2009).
- [61] G. Darrois, *Memorial des sciences mathematiques XXV, Fascicule XXV*, (Gauthier-Villars, Paris, France, 1927), chap. V.
- [62] W. Israel, *Nuovo Cimemto* 44, 1 (1966)
- [63] W. Israel, *Nuovo Cimemto* 48, 463(E) (1967).
- [64] K. Lanczos, *Ann. Phys.* 379, 518 (1924).
- [65] E. Poisson and M. Visser, *Phys. Rev. D* 52, 7318 (1995).
- [66] F. S. N. Lobo and P. Crawford, *Class. Quantum Gravity* 21, 391 (2004).